

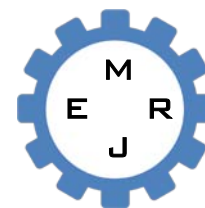


Dept. of Mech. Eng.
CUET

Published Online March 2015 (<http://www.cuet.ac.bd/merj/index.html>)

Mechanical Engineering Research Journal

Vol. 9, pp. 66–71, 2013



ISSN: 1990-5491

RENEWABLE HYDROGEN FROM AQUEOUS PHASE REFORMING (APR) OF GLYCEROL

M. M. Rahman^{1*}, R. K. Opu² and B. Salam¹

¹Dept. of Mechanical Engineering, CUET 4349, Bangladesh

²Dept. of Civil Engineering, RUET 6204, Bangladesh

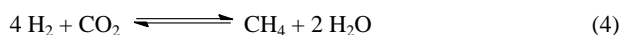
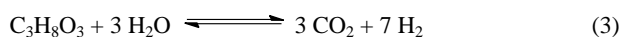
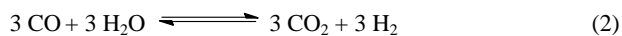
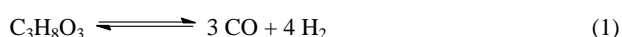
Abstract: In this study a series of Pt-Ni composites were supported on alumina doped with 3 wt% ceria, and the resulting materials were characterized and tested as catalysts for the aqueous phase reforming of glycerol to produce H₂. Amongst the catalysts tested, bimetallic 1Pt-6Ni/3CeAl catalyst gave the highest H₂ yield (86%) and gas phase C yield (94%), even though it contained one third as much Pt as the benchmark 3Pt/3CeAl catalyst. Though the 3Pt/3CeAl and 1Pt-6Ni/3CeAl catalysts produced almost same amount of H₂ (1.8 and 1.9 mmol respectively) for per gram of catalyst per hour, 1Pt-6Ni/3CeAl produced five times (258 mmol) as much H₂ per gram of Pt per hour, this could make the catalyst competitive for large scale H₂ production. X-ray diffraction (XRD) and thermogravimetric (TG) analyses of the spent catalysts showed no serious catalyst deactivation by carbon deposition after 30 hour on stream, except in the case of Pt-free 6Ni/3CeAl, which ceased to produce H₂ after 15 hour on stream.

Keywords: Aqueous-phase reforming, glycerol, hydrogen, supported catalyst

1. INTRODUCTION

Although hydrogen (H₂) has the potential to become an environmentally friendly energy carrier because of its high energy density and lack of carbonaceous combustion products, its use is currently problematic in that 95% of hydrogen is produced from fossil fuels [1]. Therefore, considerable research has focused on producing H₂ from renewable sources [2]. Dumesic and co-workers pioneered the catalytic aqueous phase reforming (APR) of polyols (which can be derived from biomass) under relatively mild reaction conditions (200–250 °C, 20–50 bar) to produce a hydrogen-rich gas [3,4] that contains less CO (<300 ppm) than the product stream from conventional steam reforming does [5]. Studies examining kinetics [6] and catalyst design [3,7,8] have demonstrated that APR (shown in Eq. 1 for the case of glycerol) involves the cleavage of C–C and C–H bonds to form metal-bound surface species, especially CO, which can then react with H₂O to form H₂ and CO₂ via the water–gas shift (WGS) reaction (Eq. 2). So, the overall reaction (Eq. 3) for APR of glycerol shows that each mole of glycerol can produce maximum seven mole of hydrogen (four mole from reforming reaction and three mole from WGS reaction). Thus, a good APR catalyst must catalyze both C–C bond cleavage and

the WGS reaction [9] without promoting competing reactions such as C–O cleavage or methanation (Eq. 4), which can greatly deteriorate the yield of H₂. Group VIII metals, particularly Pt, Pd and Ni, are especially effective for APR process [10].



We recently reported that Pt supported on alumina doped with 3 wt% ceria, gave significantly higher H₂ yield and selectivity from the APR of glycerol than Pt on alumina [11]. The improved catalytic performance was attributed to their higher coking resistance and oxygen storage capacity, as well as enhanced catalysis of the WGS reaction and lower methanation activity under APR conditions. Although Pt catalysts are highly active for APR [9], the high cost of Pt makes catalysts based on non-precious metals desirable. Ni has shown initial APR activity comparable to that of Pt, but was subject to significant deactivation [10]. Thus, efforts have been made to improve the

* Corresponding author: Email: mmrahman.cuet@yahoo.com

catalytic activities of the Ni catalysts by impregnating them with other metallic elements [12]. Therefore, we synthesized Pt-Ni bimetallic catalysts supported on 3 wt% ceria-doped alumina. The ratio of Pt-Ni on the support was optimized and catalyst characterization was performed to better understand the system.

2. EXPERIMENTAL

2.1 Catalyst preparation

The 3 wt% CeO₂-Al₂O₃ supports were prepared by impregnating 2.0 g of dried (120 °C overnight) γ -Al₂O₃ (Sigma) with a solution prepared by dissolving 197 mg of (NH₄)₂[Ce(NO₃)₆] (99%, Aldrich) in 10 mL deionized water in a 100-mL glass vial. The mixture was then stirred overnight at room temperature, and the water was allowed to evaporate. The sample was then dried in air at 120 °C for 12 h and calcined under flowing air at 600 °C for 3 h (heating rate 1.5 °C/min). [Pt(NH₃)₄](NO₃)₂ (Strem Chemical) and Ni(NO₃)₂·6H₂O (Sigma-Aldrich) were dissolved, individually or together, into a minimum amount of deionized water to make monometallic or bimetallic catalysts, respectively. These were deposited on 3-wt% CeO₂-Al₂O₃ supports (3CeAl) using a conventional impregnation technique. The mixture was then stirred overnight at room temperature, and the water was allowed to evaporate. The sample was then dried in air at 120 °C for 12 h and calcined under flowing air at 600 °C for 6 h (heating rate 1.5 °C/min). Catalysts were reduced ex situ in flowing hydrogen (50 mL/min) at 800 °C for 60 min (heating rate 1.5 °C/min) at atmospheric pressure and stored under vacuum prior to use.

2.2 Catalytic test

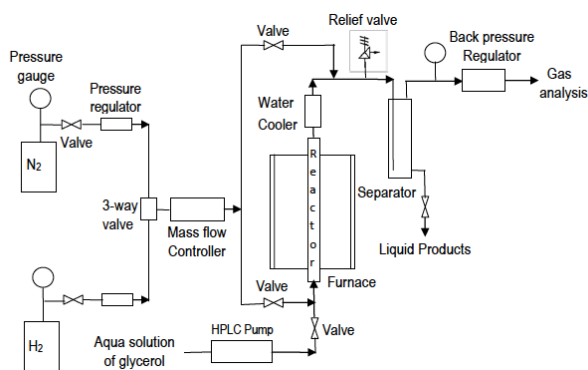


Fig. 1: Schematic of apparatus used for APR studies.

The APR of glycerol was studied in a continuous-flow fixed-bed reactor system (Fig. 1). The catalyst (250 mg) was loaded into a 5-mm i.d. stainless steel tubular reactor and held in position with quartz wool plugs. Reaction temperature was measured by a K-type thermocouple that was placed inside the reactor, very close to the catalyst bed. The reactor was mounted in a tube furnace (MTI GSL-1100X). A backpressure regulator (0 to 68 bar, Swagelok) attached to a pressure gauge was used to pressurize the system with N₂, typically at 40 bar. A 1-wt% glycerol solution was introduced using a digital hplc pump (Waters 510) at a rate of 0.05 mL/min, and heating of the catalyst

bed was initiated. When the reactor reached 240 °C, N₂ flow was set at 50 sccm using a Bronkhorst mass flow controller. The system was allowed to stabilize for about 2 h before analysis of the reaction products began. Gas products were analyzed at 25-min intervals using an online gas chromatograph (Varian CP-3800). The liquid products of the APR reaction were collected in a condenser downstream of the reactor bed, and aliquots of the condensed liquid were analyzed with a Shimadzu HPLC. Ultrapure DI water (flow rate 0.5 mL/min) was used as the eluent. The catalysts were evaluated on the bases of H₂, CO₂ and CH₄ yield, as well as carbon conversion to gas, H₂ selectivity and glycerol conversion efficiency. These were calculated according to:

$$\text{Yield of species } x = \frac{\text{moles of } x \text{ produced experimentally}}{\text{moles of } x \text{ produced theoretically}} \times 100\%$$

$$\text{C conversion to gas} = \frac{\text{moles of C in the gas products}}{\text{moles of C fed into the reactor}} \times 100\%$$

$$\text{H}_2 \text{ selectivity} = \frac{2 \times \text{moles of H}_2 \text{ produced experimentally}}{\text{Total H atoms in the gas products}} \times 100\%$$

$$\text{Glycerol conversion} = \left[1 - \frac{\text{Moles of glycerol in liquid products}}{\text{Moles of glycerol in feed}} \right] \times 100\%$$

3.1 Catalyst characterization

The textural properties of the catalysts and supports were evaluated from nitrogen adsorption-desorption isotherms at -196 °C, and the results are summarized in Table 1. The support, composed of 3 wt% CeO₂ in Al₂O₃, had S_{BET} = 162 m²/g [11]. Adding 6 wt% Ni lowered the surface area to 125 m²/g, whereas adding Pt (1 or 3 wt%) caused a smaller loss of surface area, to ~150 m²/g. As Ni was added to 1Pt/3CeAl, S_{BET} and V_p gradually decreased. D_p decreased significantly when 12 or 18 wt% Ni was present.

Table 1 Textural properties of catalysts^a

Sup ports/Catalysts	S _{BET} (m ² /g) ^b	V _p (cm ³ /g) ^c	D _p (nm) ^d
3CeO ₂ -Al ₂ O ₃ (3CeAl)	162	0.28	4.9
3Pt/3CeAl	150	0.25	4.9
1Pt/3CeAl	149	0.25	4.8
6Ni/3CeAl	125	0.22	4.9
1Pt-3Ni/3CeAl	139	0.23	4.9
1Pt-6Ni/3CeAl	120	0.20	4.9
0.5Pt-6Ni/3CeAl	122	0.22	4.9
1Pt-12Ni/3CeAl	116	0.19	4.3
1Pt-18Ni/3CeAl	109	0.18	4.3

^aMeasured by N₂ adsorption/desorption at -196°C. Prior to measurement, samples were calcined in air at 600 °C for 6 h.

^bSpecific surface area (S_{BET}) was determined from the linear portion of the isotherm (P/P₀ = 0.05–0.30) [13].

^cPore volume (V_{pore}) was calculated at P/P₀ = 0.995.

^dPredominant pore size (volume basis) (D_{pore}) was calculated from the adsorption isotherm using the Barrett-Joyner-Halenda (BJH) formula [14].

Fig. 2 shows the XRD patterns of the catalysts following reduction at 800 °C. These demonstrated that NiO was completely reduced to Ni⁰, with diffraction peaks at 2θ = 44.5

and 51.8° corresponding to the (111) and (200) planes, respectively of Ni [15]. The amount of detectable crystalline Ni⁰ and the particle size of metallic Ni increased with increasing Ni content. The catalyst with 1 wt% Pt and 6 wt% Ni showed the lowest Pt⁰ peak intensity and greatest peak width at half height, which could indicate that dispersion was highest at this Pt-Ni mixing ratio. A shift in the diffraction peak representing the Pt (111) reflection ($\Delta(2\theta) = +0.15^\circ$) was noted in the 1Pt-18Ni/3CeAl sample compared to the 3Pt/3CeAl (Fig. 2). This could indicate the formation of solid solution of Pt and Ni [16]; though the breadth of the peak in the XRD pattern of the former sample prohibits quantitative analysis.

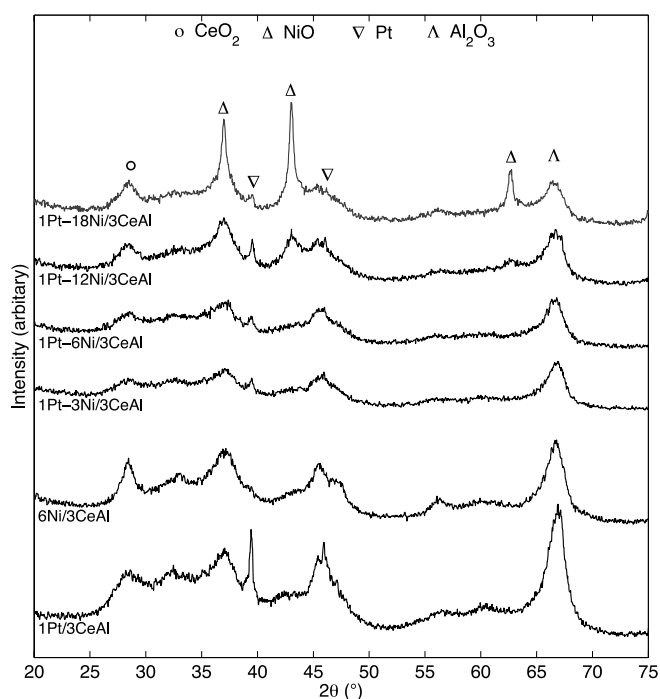


Fig. 2: X-ray diffraction patterns of catalysts that had been reduced in flowing H₂ (50 vol.% in N₂) at 800 °C for 60 min (heating rate 1.5 °C/min). 3Pt/3CeAl and 1Pt/3CeAl were reduced at 500 °C.

Also EDS analysis of 1Pt-18Ni/3CeAl catalyst confirmed that Ni and Pt coexisted on some areas of the support [17], as shown in Fig. 3. Even though no alloying effect was observed from temperature programmed reduction (TPR) but X-ray photoelectron spectra (XPS) analysis showed a significant peak shift of Pt, indicating an electronic interaction between Pt and Ni.

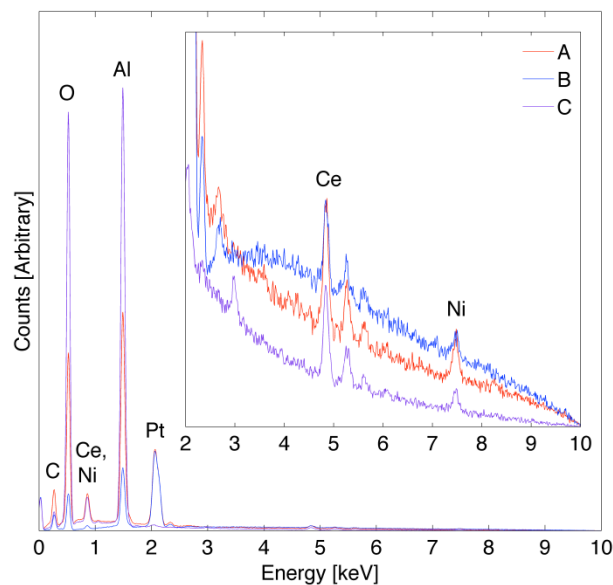
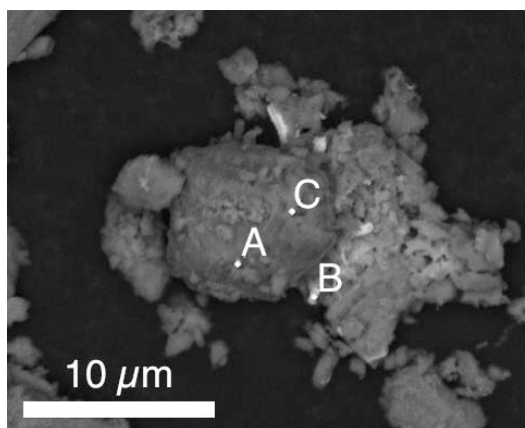


Fig. 3: EDS spectra of 1Pt-18Ni/3CeAl catalysts that were reduced in flowing H₂ (50 vol% in N₂) at 800 °C for 60 min (heating rate 1.5 °C/min).

3.2 Activity tests

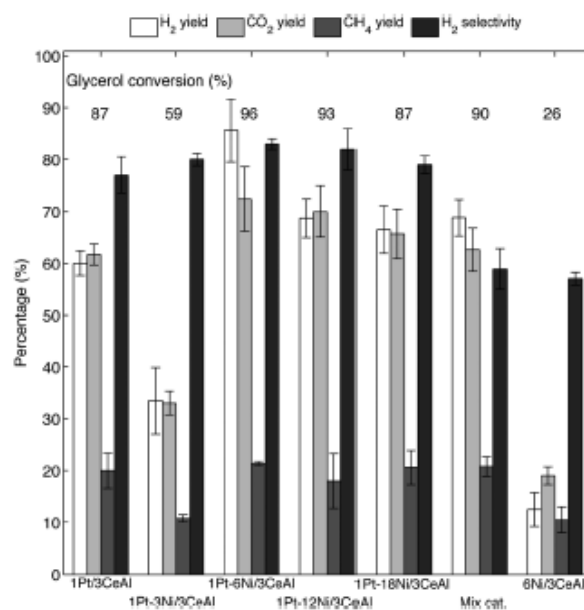


Fig. 4: Effect of Ni addition to Pt/3CeAl catalysts on the yields, gas phase conversions and feed conversions in the aqueous phase reforming of glycerol (240 °C, 40 bar, 1 wt% glycerol, 0.05 mL/min, 250 mg catalyst; data are mean values over $t = 5-20$ h). Error bars indicate one standard deviation; each bar is the average of ≥ 2 experiments.

An aqueous solution with 1 wt% glycerol was used to evaluate the performance of the catalysts. All reactions were performed at 240 °C, 40 bar, and with a feed flow rate of 0.05 mL/min, irrespective of the catalyst used. The reaction data presented in Fig. 4 shows that the aqueous-phase reforming of glycerol over any of the studied catalysts indeed leads to a hydrogen-rich gas phase. Alkanes larger than methane (i.e ethane) were only detected in trace amounts and were not further quantified. No CO was detected, indicating that CO

concentration in the product gas was below the GC detection limit (i.e. $[\text{CO}] \leq 100$ ppm) in all reactions. The H_2 yield from the APR of glycerol was calculated as the ratio of the amount of H_2 produced divided by the amount of H_2 that could have been produced if all of the glycerol was completely reformed to H_2 and CO_2 (according to the stoichiometric reaction for APR of glycerol, 1 mol of glycerol produces 7 mol of H_2 (Eq. 3) [9]). The H_2 yields (Fig. 4) and H_2 concentrations in the products from glycerol reforming over three of the nickel-containing catalysts, 1Pt-6Ni/3CeAl, 1Pt-12Ni/3CeAl and 1Pt-18Ni/3CeAl, were similar to those obtained over 3Pt/3CeAl (78 and 69%, respectively), despite that these catalysts contained one third as much Pt. Among these three nickel-containing catalysts, the H_2 yield decreased with increasing Ni loading. Thus the highest H_2 yield (86%) and selectivity (83%) were observed for APR over 1Pt-6Ni/3CeAl; whereas the lowest H_2 yield (13%) and H_2 selectivity (57%) was observed over Pt-free 6Ni/3CeAl. Notably, the APR of glycerol over 1Pt-6Ni/3CeAl, 1Pt-12Ni/3CeAl and 1Pt-18Ni/3CeAl produced more CO_2 than that over 3Pt/3CeAl (Fig. 4), and the bimetallic catalysts gave gas products richer in CO_2 . This is consistent with the higher activity of Ni as a WGS catalyst (Eq. 2) [18], and may help to explain why similar H_2 yields were generated by these catalysts and by 3Pt/3CeAl, despite their much lower Pt content. Using less than 1 wt% Pt or less than 6 wt% Ni (as in 1Pt-3Ni/3CeAl, 0.5Pt-6Ni/3CeAl and 6Ni/3CeAl) significantly lowered catalytic activity for the APR of glycerol. Despite that Ni favors methanation [19], the APR of glycerol over 1Pt-6Ni/3CeAl, 1Pt-12Ni/3CeAl and 1Pt-18Ni/3CeAl showed similar CH_4 yields to the reaction over 3Pt/3CeAl (19%). This could be due to an interaction between Pt and Ni; a bimetallic interaction between Pt and Cu has been credited for lowering methane production in the APR of glycerol over magnesium/aluminium oxides [20]. Nevertheless, the highest fraction of CH_4 in the gas product (32%) was obtained using 6Ni/CeAl as the catalyst.

The liquid phase was also analyzed after the reaction over each of the catalysts. Apart from unreacted glycerol, traces of some other compounds, particularly ethanol and propylene glycol, were identified, but were not further quantified. The conversions of glycerol, gas phase C yields, and rates of each reaction are shown in Table 2. The APR of 1 wt% glycerol over catalysts 1Pt-6Ni/3CeAl, 1Pt-12Ni/3CeAl and 1Pt-18Ni/3CeAl produced similar glycerol conversion efficiencies and gas phase carbon yields as that over 3Pt/3CeAl, with both quantities decreasing as the Ni content increased from 6 to 18 wt%. Without Pt, i.e. when the catalyst was 6Ni/3CeAl, catalytic performance was poor, likely due to the oxidation of Ni particles after 15 h on-stream under the hydrothermal conditions used for APR. For the catalysts 1Pt-3Ni/3CeAl, 0.5Pt-6Ni/3CeAl, and 6Ni/3CeAl, the main liquid phase product was unreacted glycerol; these produced less ethanol and acetic acid than the 3Pt/3CeAl catalyst. Compared to the monometallic 1Pt/3CeAl and 6Ni/3CeAl catalysts, the bimetallic 1Pt-6Ni/3CeAl, 1Pt-12Ni/3CeAl and 1Pt-18Ni/3CeAl catalysts showed much higher glycerol conversion and gas phase C yield. To evaluate

catalytic activity, reaction rate has been calculated based on moles of glycerol per hour per gram of Pt metal. Though the alloying effect of Pt and Ni can greatly increase the conversion of the APR reaction, also the co-existence of individual Pt and Ni nanoparticles can greatly increase the conversion of the APR reaction, in good accordance with the literature [21]. Amongst all catalysts tested, 3Pt/3CeAl showed the lowest (0.14 mol gPt⁻¹ h⁻¹) and 1Pt-6Ni/3CeAl the highest (0.41 mol gPt⁻¹ h⁻¹) activity. As the Ni loading increased from 6 to 18 wt%, the reaction rate decreased gradually.

Table 2: Conversion and reaction rate in the APR of glycerol over ceria/alumina-supported catalysts^a

Catalysts	Gly. Conv. (%)	Gas phase C yield (%)	Reaction rate (mol gPt ⁻¹ h ⁻¹) ^b
3Pt/3CeAl	95	82	0.14
1Pt/3CeAl	87	80	0.37
1Pt-3Ni/3CeAl	59	44	0.25
1Pt-6Ni/3CeAl	96	94	0.41
0.5Pt-6Ni/3CeAl	47	34	0.20
1Pt-12Ni/3CeAl	93	88	0.39
1Pt-18Ni/3CeAl	87	86	0.38
6Ni/3CeAl	26	24	-

^aAqueous-phase reforming of glycerol at 240 °C under 40 bar N_2 . Values are calculated based on data collected over $t = 5$ –20 h.

^bReaction rate refers to the rate of glycerol consumption at 240 °C: 40 bar.

Two main causes of catalyst deactivation in APR are carbon deposition and the sintering of the active metal [12]. Figure 8 presents the XRD patterns of the fresh and spent xPt-yNi/3CeAl catalysts. No carbon formation [22], expected at $2\theta = 25.5^\circ$, was observed on the spent catalysts after 30 h on-stream. None of the spent 1Pt-18Ni/3CeAl, 1Pt-12Ni/3CeAl, or 1Pt-6Ni/3CeAl catalysts showed XRD peaks for NiO; rather, they showed two clear NiO peaks at 44.5 and 51.8°. This was expected, as Pt prevents the oxidation of Ni [17]. However, no Ni peak was observed in the XRD patterns of spent 6Ni/3CeAl, which instead showed clear diffraction lines for NiO at $2\theta = 37.2$ and 62.9 [15]. Thus the Ni particle was oxidized to NiO, consistent with the complete loss of activity observed. In addition, the peak for γ -Al₂O₃ at $2\theta = 66.7^\circ$ was sharper in the XRD patterns of the fresh than the spent catalysts; this peak broadening may have been caused by the reduction of the support and deposition of carbon and coke-like materials. The other new peak identified in the patterns of the spent high-Ni catalysts ($2\theta = 28.18^\circ$, SP. 1Pt-18Ni/3CeAl, SP. 1Pt-12Ni/3CeAl, Fig. 8), may indicate the presence of NiOOH (JCPDS 27-0956; $2\theta = 28.16^\circ$). This could have formed upon the reaction of Ni, or even NiO produced in situ, with H_2O .

Thermogravimetric analysis of the spent catalysts under flowing instrument air showed several mass-loss events. Most catalysts did not lose mass upon heating to 1000 °C, indicating that no coke (which would have been burned to CO_2) was deposited on the catalyst surfaces. The exception was the catalyst mixture, which showed significant weight loss due to the burning of coke at 550 °C. However, on the least-active catalysts, 6Ni/3CeAl, 0.5Pt-6Ni/3CeAl and 1Pt-3Ni/3CeAl,

some weight loss occurred at ~ 290 °C; this could have been due to the oxidation of amorphous carbon or the condensation of surface hydroxyl groups to release water. Catalyst deactivation (6Ni/3CeAl) is consistent with the build up of amorphous C, small amounts of which would be difficult to observe by XRD. As no such combustion events were observed when the catalysts with at least 1 and 6 wt% Pt and Ni, respectively, were analyzed after use, we conclude that the TGA peak at 290 °C was due to amorphous carbon, but that 1 wt% Pt, when co-precipitated on 3CeAl, was sufficient to stabilize 6 wt% Ni (Fig. 5).

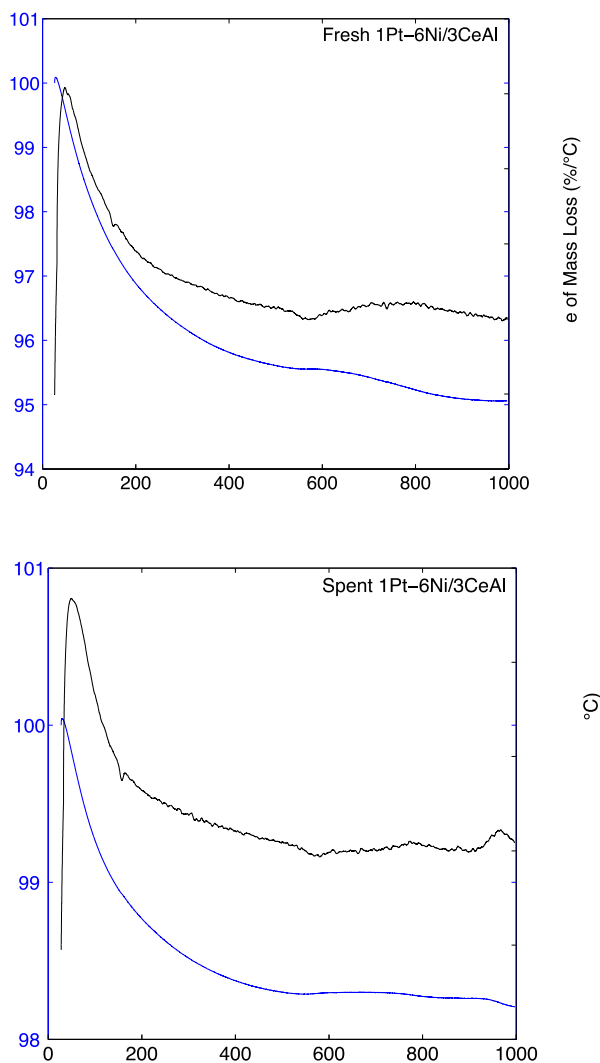


Fig. 5: Thermogravimetric analysis of fresh (reduced: 50 vol.% H₂ in N₂, 800 °C, 60 min) and spent (after reaction: 240 °C, 40 bar, 1 wt% glycerol, 0.05 mL/min, 30 h) 1Pt-6Ni/3CeAl catalyst.

4. CONCLUSIONS

In the APR of glycerol, 3Pt/3CeAl catalyst showed good activity and selectivity towards H₂ production compared to 3Pt/Al [11]. Although Pt catalysts are highly active for APR, the high cost of Pt makes catalysts based on non-precious metals desirable. A bimetallic Pt-Ni catalyst showing good activity for the APR of glycerol to produce H₂ was developed in this work. Bimetallic 1Pt-6Ni/3CeAl showed the highest H₂ yield and gas phase C yield, even though it contained one third as much Pt as

the monometallic catalyst, 3Pt/3CeAl. Though 3Pt/3CeAl and 1Pt-6Ni/3CeAl produced almost same amount of H₂ per gram of catalyst per hour, 1Pt-6Ni/3CeAl produced five times as much H₂ per gram of Pt. XRD and TGA analysis of spent catalysts showed no serious deactivation by carbon deposition after 30 hour on-stream, except in the case of 6Ni/3CeAl, which had ceased to produce detectable H₂ after 15 hours.

REFERENCES

- [1] B. C. R. Ewan and R. W. K. Allen, "A figure of merit assessment of the routes to hydrogen", *Int. J. Hydrogen Energy*, Vol. 30, pp. 809–819, 2005.
- [2] S. Dunn, "Hydrogen futures: toward a sustainable energy system", *Int. J. Hydrogen Energy*, Vol. 27, pp. 235–264, 2002.
- [3] R. D. Cortright, R. R. Davda and J. A. Dumesic, "Hydrogen from catalytic reforming of biomass-derived hydrocarbons in liquid water", *Nature*, Vol. 418, pp. 964–967, 2002.
- [4] G. W. Huber, R. D. Cortright and J. A. Dumesic, "Renewable Alkanes by Aqueous-Phase Reforming of Biomass-Derived Oxygenates", *Angew. Chem. Int. Ed.*, Vol. 43, pp. 1549–1551, 2004.
- [5] G. W. Huber, J. W. Shabaker, S. T. Evans and J. A. Dumesic, "Aqueous-phase reforming of ethylene glycol over supported Pt and Pd bimetallic catalysts", *Appl. Catal., B*, Vol. 62, pp. 226–235, 2006.
- [6] J. W. Shabaker, G. W. Huber, R. R. Davda, R. D. Cortright and J. A. Dumesic, "Aqueous-Phase Reforming of Ethylene Glycol Over Supported Platinum Catalysts", *Catal. Lett.*, Vol. 88, pp. 1–8, 2003.
- [7] S. Adhikari, S. D. Fernando and A. Haryanto, "Hydrogen production from glycerin by steam reforming over nickel catalysts", *Renewable Energy*, Vol. 33, pp. 1097–1100, 2008.
- [8] R. R. Soares, D. A. Simonetti, J. A. Dumesic, "Glycerol as a Source for Fuels and Chemicals by Low-Temperature Catalytic Processing", *Angew. Chem. Int. Ed.*, Vol. 45, pp. 3982–3985, 2006.
- [9] R. R. Davda, J. W. Shabaker, G. W. Huber, R. D. Cortright and J. A. Dumesic, "A review of catalytic issues and process conditions for renewable hydrogen and alkanes by aqueous-phase reforming of oxygenated hydrocarbons over supported metal catalysts", *Appl. Catal., B*, Vol. 56, pp. 171–186, 2005.
- [10] R. R. Davda, J. W. Shabaker, G. W. Huber, R. D. Cortright and J. A. Dumesic, "Aqueous-phase reforming of ethylene glycol on silica-supported metal catalysts", *Appl. Catal., B*, Vol. 43, pp. 13–26, 2003.
- [11] T. L.C., M. M. Rahman, Andrew I. Minett, and Andrew T. Harris, "Effect of ceria addition to the alumina supports of Pt catalysts on the aqueous-phase reforming of glycerol", *ChemSusChem*, (2013 Accepted for publication).
- [12] J. W. Shabaker, G. W. Huber and J. A. Dumesic,

- “Aqueous-phase reforming of oxygenated hydrocarbons over Sn-modified Ni catalysts”, *J. Catal.*, Vol. 222, pp. 180–191, 2004.
- [13] S. Brunauer, P. H. Emmett and E. Teller, “Adsorption of Gases in Multimolecular Layers”, *J. Am. Chem. Soc.*, Vol. 60, pp. 309–319, 1938.
- [14] E. P. Barrett, L. G. Joyner and P. P. Halenda, “The determination of pore volume and area distributions in porous substances. I. Computations from nitrogen isotherms”, *J. Am. Chem. Soc.*, Vol. 73, pp. 373–380, 1951.
- [15] A. Iriondo, V. L. Barrio, J. F. Cambra, P. L. Arias, M. B. Güemez, R. M. Navarro, M. C. Sánchez-Sánchez and J. L. G. Fierro, “Hydrogen Production from Glycerol Over Nickel Catalysts Supported on Al₂O₃ Modified by Mg, Zr”, Ce or La, *Top Catal.*, Vol. 49, pp. 46–58, 2008.
- [16] A. Tegou, S. Papadimitriou, I. Mintsouli, S. Armyanov, E. Valova, G. Kokkinidis and S. Sotiropoulos, “Rotating disc electrode studies of borohydride oxidation at Pt and bimetallic Pt–Ni and Pt–Co electrodes”, *Catal. Today*, Vol. 170, pp. 126–133, 2011.
- [17] A. Tanksale, J. N. Beltramini, J. A. Dumesic and G. Q. Lu, “Effect of Pt and Pd promoter on Ni supported catalysts—A TPR/TPO/TPD and microcalorimetry study”, *J. Catal.*, Vol. 258, pp. 366–377, 2008.
- [18] D. C. Grenoble, M. M. Estadt and D. F. Ollis, “The chemistry and catalysis of the water gas shift reaction: 1. The kinetics over supported metal catalysts”, *J. Catal.*, Vol. 67, pp. 90–102, 1981.
- [19] M. A. Vannice, “The catalytic synthesis of hydrocarbons from H₂CO mixtures over the Group VIII metals: V. The catalytic behavior of silica-supported metals”, *J. Catal.*, Vol. 50, pp. 228–236, 1977.
- [20] D. A. Boga, R. Oord, A. M. Beale, Y. M. Chung, P. C. A. Bruijninx and B. M. Weckhuysen, “Highly Selective Bimetallic Pt–Cu/Mg(Al)O Catalysts for the Aqueous-Phase Reforming of Glycerol”, *CHEMCATCHEM*, Vol. 5, pp. 529–537, 2013.
- [21] X. Wang, N. Li, L. D. Pfefferle and G. L. Haller, “Pt–Co bimetallic catalyst supported on single walled carbon nanotube: XAS and aqueous phase reforming activity studies”, *Catal. Today*, Vol. 146, pp. 160–165, 2009.
- [22] J. Comas, F. Mariño, M. Laborde, N. Amadeo, “Bio-ethanol steam reforming on Ni/Al₂O₃ catalyst”, *Chem. Eng. J.*, Vol. 98, 61–68, 2004.